

# Profit-Oriented BESS Siting and Sizing in Deregulated Distribution Systems

Xiaofei Wang<sup>1</sup>, Graduate Student Member, IEEE, Fangxing Li<sup>2</sup>, Fellow, IEEE, Qiwei Zhang<sup>1</sup>, Graduate Student Member, IEEE, Qingxin Shi, Member, IEEE, and Jinning Wang, Graduate Student Member, IEEE

**Abstract**—Within the deregulation process of distribution systems, the distribution locational marginal price (DLMP) provides effective market signals for future unit investment. In that context, this paper proposes a two-stage stochastic bilevel programming (TS-SBP) model for investors to best allocate battery energy storage systems (BESSs). The first stage obtains the optimal siting and sizing of BESSs on a limited budget. The second stage, a bilevel BESS arbitrage model, maximizes the arbitrage revenue in the upper level and clears the distribution market in the lower level. Karush-Kuhn-Tucker (KKT) optimality conditions, strong duality theory, and the big-M method are utilized to transform the TS-SBP model into a tractable two-stage stochastic mixed-integer linear programming (TS-SMILP) model. A novel statistics-based scenario extraction algorithm is proposed to generate a series of typical operating scenarios. Then, scale reduction strategies for BESS candidate buses and inactive voltage constraints are proposed to reduce the scale of the TS-SMILP model. Finally, case studies on the IEEE 33-bus and 123-bus systems validate the effectiveness of the DLMP in incentivizing BESS planning and the efficiency of the two proposed scale reduction strategies.

**Index Terms**—Distribution locational marginal price (DLMP), siting and sizing, scenario extraction, two-stage stochastic bilevel programming (TS-SBP), scale reduction, battery energy storage systems (BESSs).

## NOMENCLATURE

### Sets

$\Omega_T$	Set of time slots
$\Omega_G$	Set of generators, $\Omega_G = \Omega_{MT} \cup \Omega_{SVC}$
$\Omega_{MT}$	Set of MTs
$\Omega_{SVC}$	Set of SVCs
$\Omega_N$	Set of buses
$\Omega_{BS}$	Set of candidate buses for BESS installation

$\Omega_V$	Set of buses at which voltage constraints can be maintained
$S$	Set of scenarios.

### Constants

$c^{Mf}/c^{Mv}$	Fixed/variable O&M cost
$N_{BS}^{\max}$	Maximal number of BESSs
$k^p/k^e$	Fixed power/energy cost for installing a BESS
$C^{Bgt}$	Budget limit
$P^{\min}/P^{\max}$	Minimum/maximum rated power of a BESS
$E^{\min}/E^{\max}$	Minimum/maximum rated energy of a BESS
$p(s)$	Probability of scenario $s$
$\eta_i$	Round-trip efficiency of BESS $i$
$SOC_i^{\min}/SOC_i^{\max}$	Minimum/maximum SOC of BESS $i$
$\sigma_{sub,t}^{p,s}/\sigma_{sub,t}^{q,s}$	Active/reactive LMP of the substation at time $t$
$\sigma_{i,t}^{p,s}/\sigma_{i,t}^{q,s}$	Active/reactive bidding price of generator $i$ at time $t$
$P_{i,t}^{D,s}/Q_{i,t}^{D,s}$	Fixed active/reactive load demand of bus $i$ at time $t$
$V^{\min}/V^{\max}$	Minimum/maximum voltage limits
$V_{sub,t}^s$	Voltage of the substation at time $t$
$P_i^{G,\min}/P_i^{G,\max}$	Minimum/maximum active power of generator $i$ at time $t$
$Q_i^{G,\min}/Q_i^{G,\max}$	Minimum/maximum reactive power of generator $i$ at time $t$
$\alpha_i$	Power factor of generator $i$
$Z^P/Z^q$	Matrices of nodal voltage change concerning net active/reactive power injection.

### Variables

$P_i^{\text{rated}}/E_i^{\text{rated}}$	Rated power/energy of BESS $i$
$\delta_i$	Binary variable indicating whether a BESS is installed at bus $i$
$\pi_{i,t}^s$	Active DLMP of node $i$ at time $t$
$P_{i,t}^{c,s}/P_{i,t}^{d,s}$	Charging/discharging power of BESS $i$ at time $t$
$P_{i,t}^{BESS,s}$	Power exchange of BESS $i$ at time $t$ with the power grid
$E_{i,t}^s$	Energy stored in BESS $i$ at time $t$

Manuscript received 24 August 2021; revised 7 December 2021; accepted 23 January 2022. Date of publication 11 February 2022; date of current version 20 February 2023. This work was supported in part by the U.S. National Science Foundation via under Award ECCS-1809458. Paper no. TSG-01353-2021. (Corresponding author: Fangxing Li.)

Xiaofei Wang, Fangxing Li, Qiwei Zhang, and Jinning Wang are with the Department of EECS, The University of Tennessee, Knoxville, TN 37996 USA (e-mail: fli6@utk.edu).

Qingxin Shi is with the College of Electrical and Electronics Engineering, North China Electric Power University, Beijing 102206, China.

Color versions of one or more figures in this article are available at <https://doi.org/10.1109/TSG.2022.3150768>.

Digital Object Identifier 10.1109/TSG.2022.3150768

$P_{sub,t}^{G,s}/Q_{sub,t}^{G,s}$	Active/reactive power drawn from the wholesale market at time $t$
$P_{i,t}^{G,s}/Q_{i,t}^{G,s}$	Active/reactive power of generator $i$ at time $t$
$P_t^{L,s}/Q_t^{L,s}$	Active/reactive power loss at time $t$
$V_{j,t}^s$	Voltage of bus $j$ at time $t$
$\lambda_t^{p,s}/\lambda_t^{q,s}$	Lagrangian multipliers associated with active/reactive equality power constraints
$\omega_{i,t}^{(\cdot) \min,s}/\omega_{i,t}^{(\cdot) \max,s}$	Lagrangian multipliers associated with inequality voltage and active/reactive power constraints
$\kappa_{i,t}^{-,s}/\kappa_{i,t}^{+,s}$	Lagrangian multipliers associated with inequality reactive power constraints.

## I. INTRODUCTION

**T**RADITIONALLY, a power system has a unidirectional structure where electricity is generated by generators and then delivered via transmission and distribution lines to consumers, who are at the end of the supply chain. However, over the last 20 years, the electricity industry has witnessed the emergence of distributed energy resources (DERs) in distribution systems [1]. The proliferation of DERs has transformed the unidirectional system into a bidirectional system, making the distribution system more flexible and more active, and also more complex. To take advantage of these new opportunities and to keep pace with deregulation in power distribution systems, the concept of a distribution market has been proposed and widely studied [2], [3].

The distribution locational marginal price (DLMP), the extension of locational marginal price (LMP) to distribution networks, has been proposed to either guide the consumption of flexible loads, or act as the bidding price of DERs when participating in the distribution market. In [4], [5], the DLMP varies throughout the course of a day and is utilized to optimize the charging schedule for electric vehicles (EVs) and household demand response to alleviate congestion issues. In [6], the DLMP is regarded as both the microgrid (MG) bidding price and the clearing price of the distribution system operator (DSO). A bilevel model is built and a strategic bidding strategy is proposed to maximize MG profits. A similar bi-level model is proposed in [7] to achieve optimal EV aggregator scheduling.

The above studies mainly focus on short-term operations. However, the DLMP also releases continuous and effective market signals to practitioners, which can incentivize future DERs investment. Among all types of DERs, the battery energy storage system (BESS) plays a significant role due to both its flexible charging/discharging characteristic and its increasing penetration level. Between 2011 and 2020, the Federal Energy Regulatory Commission (FERC) Orders No. 755 [8], 841 [9] and 2222 [10] have gradually removed the barriers to BESS participation in the energy and ancillary market. In the industry field, various related trading products, such as CAISO's flexible ramping product [11] and PJM's Regulation D [12], have promoted the deployment of BESSs. The cost of BESSs also continues to decrease as technology advances. All of these advantages are driving the acceleration of BESS

installation, which is likely to continue into the foreseeable future [13]. In this context, the optimal allocation of BESSs has already been extensively studied.

In normal operating conditions, the optimal allocation of BESSs or distributed generators (DGs) traditionally aimed to either 1) minimize the investment cost and the long-term cumulative operating cost of distribution systems, or 2) to satisfy the system operating conditions (e.g., meeting load growth, improving voltage profile and reducing power losses), usually from the viewpoint of the DSO or a utility [14]–[18]. In [14], a stochastic mixed-integer linear programming (MILP) model was formulated to optimally site and size BESSs to minimize both the system operating cost and the BESS investment cost. The optimal placement and sizing of energy storage (ES) to minimize total energy losses was studied in [15]. A single-level mixed-integer second-order cone programming (MISOCP) model was established in [16] to determine the optimal siting and sizing for BESSs. Reference [17] determined the optimal BESS allocation to maximize net revenue. The same problem in an imbalanced system was further studied in [18]. Reference [19] aimed to characterize the economic effect of ES geometrically and investigate the optimal energy-power ratio for ES.

These studies were performed in a regulated distribution system. However, in deregulated distribution systems, the planning objective and investment goal differ from the regulated case because of the profitability of private DER owners. Considering the characteristics of electricity prices in competitive distribution systems, such as the spatial and temporal difference of the DLMP, private DER owners are motivated to install DERs at optimal locations in optimal sizes to maximize profits.

A few studies have been developed in this background. The authors in [20] proposed a bi-level wind-storage expansion model to maximize investor profits in the transmission level market, in which only the capacity was optimized. In [21], a three-stage model for network reinforcement and DERs planning was proposed. The objective was to maximize asset owners' profit by optimizing the location and construction time of new lines or DERs. In the third stage, the DLMP was utilized as the market signal to modify the planning in the first two stages. In [22], MGs were assumed to trade with the DSO. MG locations were based on the weighted sum of loss sensitivity factors and voltage sensitivity factors. The installation time and DER type were determined by solving a bilevel model with the DSO in the upper level and MGs in the lower level. Reference [23] determined the optimal sizes for renewable generators and ES in a deregulated market with given candidate sites. An adaptive robust model for investment planning of DERs was proposed in [24], in which the 8760-hour operating conditions in each planning year were clustered to a tractable count. In [25], with the constraint of wind turbines (WTs) of a fixed size, an exhaustive search method was proposed to find the most convenient WT allocations and the priority of installations.

In the above studies, electricity price and earned profit have been proposed and deployed to motivate system investment. These studies have provided some insights for planning in

a distribution market environment. However, there are still important issues that have not been well addressed in the literature: 1) Daily day-ahead market clearing is seldom considered, as shown in [22], [24] in which the operating conditions are reduced or clustered to a low resolution, not to a consecutive 24 hours. 2) The methods proposed in previous studies may not be suitable for BESS planning since the daily operating constraints for BESSs cannot be included, such as constraint (10) in Section II-B. 3) In [22]–[25], as an indicator of the physical operating conditions, the DLMP is not fully modeled or utilized, meaning that its potential in incentivizing system planning can be further explored.

To fill these gaps, this paper focuses on the optimal siting and sizing of BESSs for private investors. This planning is formulated as a two-stage stochastic bilevel programming (TS-SBP) problem. The first stage determines the locations, sizes, and number of BESSs within a limited budget. The second stage maximizes investors' arbitrage profits over long-term operation, which is modeled as a bi-level problem with the investors in the upper level and the DSO in the lower level. The contributions of this paper are summarized as follows:

1) The DLMP is applied as a price signal to incentivize BESS planning in a deregulated distribution system. The proposed planning approach maximizes investor profit and improves system operating conditions, which is aligned with the incentive compatibility that benefits both the BESS owners and the distribution system.

2) A TS-SBP arbitrage model is established, in which the planning stage and the operating stage are combined as a two-stage problem, and the operating stage is formulated as a bi-level problem. The objective of the TS-SBP model is to minimize maintenance costs and maximize arbitrage revenue.

3) From the 1-year historical LMP and system load dataset, a  $k$ -means-based scenario extraction algorithm is proposed to extract the most representative patterns of a consecutive 24 hours LMP, as well as system load profiles and their corresponding discrete joint probabilities. The extraction accuracy is validated, and this innovation enables day-ahead market clearing.

4) Based on the unique characteristics of this problem, such as the limited number of BESSs to be installed and the huge number of inactive constraints, two scale-reduction strategies, BESS candidate buses reduction and inactive voltage constraints reduction, are proposed to reduce computational complexity for this large-scale optimization problem. The simulation results demonstrate the accuracy of these strategies.

It should be noted that this work addresses profit-oriented BESS planning, which is appropriate for areas where resilience is not a considerable concern. However, in areas with resilience as a significant concern such as coastal regions prone to extreme weather like hurricanes, the problem may follow a fundamentally different model with resilience as a major factor; that is a problem for a future work to investigate.

The rest of this paper is organized as follows. Section II describes the TS-SBP model. Section III proposes the scenario extraction algorithm. Section IV presents the solution methods and two scale-reduction strategies. Section V presents case studies. Section VI concludes the paper.

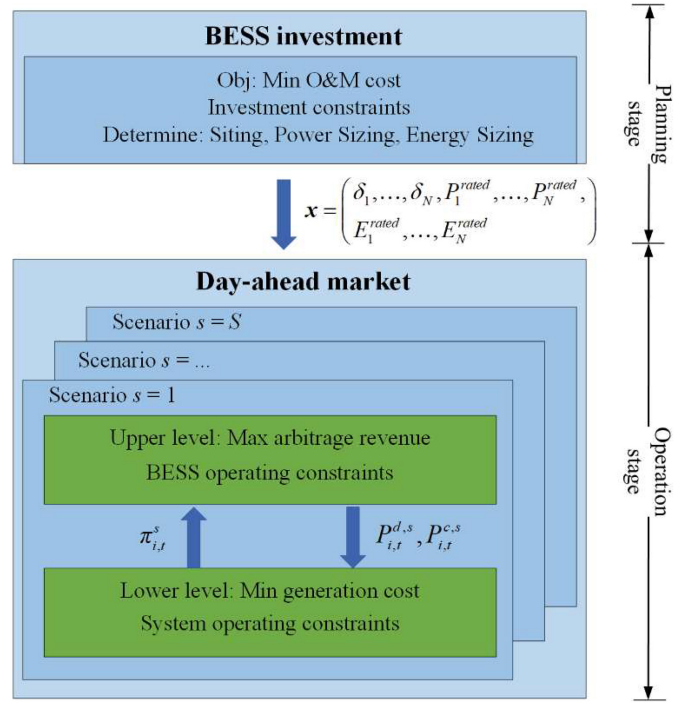


Fig. 1. The framework of the TS-SBP model.

## II. PROBLEM FORMULATION

The mathematical formulation of the TS-SBP model is presented in this section. The overall framework is shown in Fig. 1.

### A. The First Stage Problem: Optimal Siting & Sizing

The first stage aims to optimize the site and size of BESS units, which means private investors intend to determine the best locations and best sizes to maximize their profit.

$$\max - \sum_{i \in \Omega_{BS}} (c^{Mf} P_i^{rated} + c^{Mv} E_i^{rated}) + E[f(\mathbf{x}, s)] \quad (1)$$

$$s.t. \sum_{i \in \Omega_{BS}} \delta_i \leq N_{BS}^{\max} \quad (2)$$

$$\sum_{i \in \Omega_{BS}} k^p P_i^{rated} + k^e E_i^{rated} \leq C^{Bgt} \quad (3)$$

$$P_i^{\min} \delta_i \leq P_i^{rated} \leq P_i^{\max} \delta_i \quad (4)$$

$$E_i^{\min} \delta_i \leq E_i^{rated} \leq E_i^{\max} \delta_i \quad (5)$$

$$E_i^{rated} = 4 \cdot P_i^{rated} \quad (6)$$

$$E[f(\mathbf{x}, s)] = 365 \cdot \sum_{s \in S} p(s) f(\mathbf{x}, s) \quad (7)$$

where (1) minimizes the operation and maintenance (O&M) costs and maximizes the arbitrage revenue of the BESS over a year, the decision variables include the BESS locations, rated power, and rated energy:  $\mathbf{x} = (\delta_1, \dots, \delta_N, P_1^{rated}, \dots, P_N^{rated}, E_1^{rated}, \dots, E_N^{rated})$ , the first two items in (1) are the expression of the O&M costs; (2) restricts the number of BESSs to be installed; (3) is the investment budget limit [26], where the installation cost of a BESS is approximated as a linear function of  $P_i^{rated}$  and

$E_i^{rated}$  [27], [28]; (4) and (5) are BESS size constraints; (6) simplifies the BESS energy-power ratio to a fixed value [27]; and in (7),  $f(\mathbf{x}, s)$  is the optimal value of scenario  $s$  in the second stage problem.

### B. The Second Stage Problem: BESS Operation in a Deregulated Distribution Market

In this stage, BESSs participate in the distribution-level electricity market to maximize their arbitrage revenue. This problem has the following assumptions:

- A day-ahead electricity market is established in the distribution level. DERs provide bids and offers to the DSO, which clears the market and broadcasts the DLMP to all participants.
- BESSs are modeled as price takers that only submit load/generation quantities and the DSO decides the DLMP.

Based on these assumptions, the BESS owner and the DSO have different interests. At the same time, BESSs' charging/discharging power and system DLMP are coupled variables. Thus, a bilevel model is an appropriate representation of the coupled relationship. Note that (8)-(24) represent the scenario  $s$ . For simplicity, the expressions  $\forall t \in \Omega_T$  and  $s \in S$  behind each equation are neglected.

1) *The Upper Level:* The BESS sells energy during high DLMP hours and buys during low DLMP hours. Its objective is to maximize the arbitrage revenue.

$$\begin{aligned} f(\mathbf{x}, s) &= \max \sum_{t \in \Omega_T} \sum_{i \in \Omega_{BS}} \pi_{i,t}^s \cdot P_{i,t}^{BESS,s} \\ &= \max \sum_{t \in \Omega_T} \sum_{i \in \Omega_{BS}} \pi_{i,t}^s \cdot \left( \sqrt{\eta_i} P_{i,t}^{d,s} - P_{i,t}^{c,s} / \sqrt{\eta_i} \right) \end{aligned} \quad (8)$$

$$s.t. \quad E_{i,t+1}^s = E_{i,t}^s + P_{i,t}^{c,s} - P_{i,t}^{d,s} \quad (9)$$

$$E_{i,t=0}^s = E_{i,t=T}^s \quad (10)$$

$$SOC_i^{\min} \cdot E_i^{rated} \leq E_{i,t+1}^s \leq SOC_i^{\max} \cdot E_i^{rated} \quad (11)$$

$$0 \leq P_{i,t}^{c,s} \leq P_i^{rated}, 0 \leq P_{i,t}^{d,s} \leq P_i^{rated} \quad (12)$$

where in (8), round-trip efficiency  $\eta_i$  is used instead of using charging and discharging efficiencies [29]; (9) calculates the stored energy in the BESS with 1 hour as the time interval; (10) ensures that the daily charged and discharged energy are equal; (11) is the state of charge (SOC) constraint; (12) provides the charging and discharging power limits.

2) *The Lower Level:* The DSO clears the market intending to minimize total generation costs as well as maintain physical operating constraints.

$$\begin{aligned} \min h(z, y, s) &= \sum_{t \in \Omega_T} \left( \sigma_{sub,t}^{p,s} P_{sub,t}^{G,s} + \sigma_{sub,t}^{q,s} \widehat{Q}_{sub,t}^{G,s} \right. \\ &\quad \left. + \sum_{i \in \Omega_G} \left( \sigma_{i,t}^{p,s} P_{i,t}^{G,s} + \sigma_{i,t}^{q,s} \widehat{Q}_{i,t}^{G,s} \right) \right) \end{aligned} \quad (13)$$

$$s.t. \quad P_{sub,t}^{G,s} + \sum_{i \in \Omega_G} P_{i,t}^{G,s} + \sum_{i \in \Omega_{BS}} P_{i,t}^{BESS,s} = \sum_{i \in \Omega_N} P_{i,t}^{D,s} + P_t^{L,s} : \lambda_t^{p,s} \quad (14)$$

$$Q_{sub,t}^{G,s} + \sum_{i \in \Omega_G} Q_{i,t}^{G,s} = \sum_{i \in \Omega_N} Q_{i,t}^{D,s} + Q_t^{L,s} : \lambda_t^{q,s} \quad (15)$$

$$\begin{aligned} V_{j,t}^s &= V_{sub,t}^s + \sum_{i \in \Omega_N} Z_{j,i}^p \left( P_{i,t}^{G,s} + P_{i,t}^{BESS,s} - P_{i,t}^{D,s} \right) \\ &\quad + \sum_{i \in \Omega_N} Z_{j,i}^q \left( Q_{i,t}^{G,s} - Q_{i,t}^{D,s} \right) \end{aligned} \quad (16)$$

$$V^{\min} \leq V_{j,t}^s \leq V^{\max} : \omega_{j,t}^{v,\min,s}, \omega_{j,t}^{v,\max,s}, \forall j \in \Omega_N \quad (17)$$

$$P_i^{G,\min} \leq P_{i,t}^{G,s} \leq P_i^{G,\max} : \omega_{i,t}^{p,\min,s}, \omega_{i,t}^{p,\max,s}, \forall i \in \Omega_{MT} \quad (18)$$

$$0 \leq Q_{i,t}^{G,s} \leq P_{i,t}^{G,s} \tan(\arccos \alpha_i) : \omega_{i,t}^{q,\min,s}, \omega_{i,t}^{q,\max,s}, \forall i \in \Omega_{MT} \quad (19)$$

$$Q_i^{G,\min} \leq Q_{i,t}^{G,s} \leq Q_i^{G,\max} : \omega_{i,t}^{q,\min,s}, \omega_{i,t}^{q,\max,s}, \forall i \in \Omega_{SVC} \quad (20)$$

$$-Q_{i,t}^{G,s} \leq \widehat{Q}_{i,t}^{G,s}, Q_{i,t}^{G,s} \leq \widehat{Q}_{i,t}^{G,s} : \kappa_{i,t}^-, \kappa_{i,t}^+, \forall i \in \Omega_G \quad (21)$$

$$\begin{aligned} \pi_{i,t}^s &= \lambda_t^{p,s} + \lambda_t^{p,s} \cdot \frac{\partial P_t^{loss,s}}{\partial P_{i,t}^{D,s}} + \lambda_t^{q,s} \cdot \frac{\partial Q_t^{loss,s}}{\partial P_{i,t}^{D,s}} \\ &\quad + \sum_{j \in \Omega_N} \left( \omega_{j,t}^{v,\min,s} - \omega_{j,t}^{v,\max,s} \right) Z_{j,i}^p \end{aligned} \quad (22)$$

where (14) and (15) are active and reactive equality power constraints with the substation regarded as a large capacity generator; (16) is the linearized voltage expression derived from [2], [30]; (17) is the voltage limit; (18)-(19) are the active and reactive power limits of microturbines (MTs); (20) is the reactive power limit of static var compensators (SVCs); in (21),  $\widehat{Q}_{i,t}^{G,s} = |Q_{i,t}^{G,s}|$  since it is assumed that both absorbing and generating reactive power can induce cost [3]; and (22) is the DLMP expression derived from the Lagrangian function of this level. The power losses are linearized according to Taylor's series [2]:

$$\begin{aligned} P_t^{L,s} &\approx P_t^{L,s*} + \sum_{i \in \Omega_N} \frac{\partial P_t^{L,s}}{\partial P_{i,t}^{G,s}} \left( \Delta P_{i,t}^{G,s} - \Delta P_{i,t}^{D,s} \right) \\ &\quad + \sum_{i \in \Omega_N} \frac{\partial P_t^{L,s}}{\partial Q_{i,t}^{G,s}} \left( \Delta Q_{i,t}^{G,s} - \Delta Q_{i,t}^{D,s} \right) \end{aligned} \quad (23)$$

$$\begin{aligned} Q_t^{L,s} &\approx Q_t^{L,s*} + \sum_{i \in \Omega_N} \frac{\partial Q_t^{L,s}}{\partial P_{i,t}^{G,s}} \left( \Delta P_{i,t}^{G,s} - \Delta P_{i,t}^{D,s} \right) \\ &\quad + \sum_{i \in \Omega_N} \frac{\partial Q_t^{L,s}}{\partial Q_{i,t}^{G,s}} \left( \Delta Q_{i,t}^{G,s} - \Delta Q_{i,t}^{D,s} \right) \end{aligned} \quad (24)$$

where  $\Delta P_{i,t}^{G,s} = P_{i,t}^{G,s} - P_{i,t}^{G,s*}$  represents the power difference between two close operating points, and  $\Delta Q_{i,t}^{G,s}$ ,  $\Delta P_{i,t}^{D,s}$  and  $\Delta Q_{i,t}^{D,s}$  have similar expressions.

In (22), the DLMP is shown to consist of three components: marginal energy price, marginal power loss price, and voltage support price. The marginal energy price is determined by the bidding price of the marginal unit. The marginal power loss price reflects the power loss associated with delivering power. Since the power loss percentage in a distribution system is usually high (relative to transmission systems), it is not negligible and should be priced. Similarly, voltage is an important operating criterion and should be included. The voltage support price

represents the cost of maintaining voltage within the acceptable boundary. It is calculated using the shadow price and will be zero if there is no binding voltage constraint. The detailed analysis and discussion of the three DLMP components and their impacts on flexible loads can be found in [34].

### C. Compact Notation

To make the whole model concise and clear, a compact notation is used to elaborate the proposed TS-SBP model [31]. The first stage is:

$$\max -\mathbf{c}^T \mathbf{x} + 365 \cdot \sum_{s \in S} p(s) f(\mathbf{x}, s) \quad (25)$$

$$s.t. \mathbf{A} \mathbf{x} \leq \mathbf{b} \quad (26)$$

where  $\mathbf{x} \in \mathbb{Z}_+^{p_1} \times \mathbb{R}_+^{n_1 - p_1}$  represents the binary and continuous decision variables; (26) is the matrix representation of constraints (2)-(7) with  $\mathbf{A} \in \mathbb{R}_+^{m_1 \times n_1}$ ,  $\mathbf{b} \in \mathbb{R}_+^{m_1}$ ;  $p_1$  is the number of candidate buses;  $n_1$  is the number of total decision variables; and  $m_1$  is the number of constraints.

The second stage is given by:

$$f(\mathbf{x}, s) = \max \boldsymbol{\pi}^T \mathbf{y} \quad (27)$$

$$s.t. \mathbf{W}(s) \mathbf{y} \leq \mathbf{r}(s) - \mathbf{T}(s) \mathbf{x} \quad (28)$$

$$\boldsymbol{\pi} \in \arg \min h(\mathbf{z}, \mathbf{y}, s) \quad (29)$$

$$s.t. \mathbf{G}(s) \mathbf{z} \leq \mathbf{e}(s) - \mathbf{K}(s) \mathbf{y} \quad (30)$$

where  $\mathbf{y} \in \mathbb{R}_+^{n_2}$ ,  $\boldsymbol{\pi} \in \mathbb{R}_+^{n_2}$ ,  $\mathbf{W} \in \mathbb{R}_+^{m_2 \times n_2}$ ,  $\mathbf{r} \in \mathbb{R}_+^{m_2}$ ,  $\mathbf{T} \in \mathbb{R}_+^{m_2 \times n_1}$ ,  $\mathbf{z} \in \mathbb{R}_+^{n_3}$ ,  $\mathbf{G} \in \mathbb{R}_+^{m_3 \times n_3}$ ,  $\mathbf{e} \in \mathbb{R}_+^{m_3}$ ,  $\mathbf{K} \in \mathbb{R}_+^{m_3 \times n_2}$ .

## III. SCENARIO EXTRACTION AND VARIABLE NODAL LOADS

The DLMP plays an important role in the TS-SBP planning problem. In the meantime, the DLMP is significantly influenced by the wholesale market LMP and the distribution system load. However, because the LMP and load vary every hour and every day, applying all historical data will significantly increase the computational burden, making this problem intractable. Thus, a natural alternative is to extract a series of representative operating scenarios from the historical dataset, which are defined as possible LMP profile and system load profile combinations in this study.

### A. Scenario Extraction

The statistics-based scenario extraction includes three steps: historical LMP and load clustering, scenario generation, and scenario reduction. The detailed procedures are shown in Algorithm 1.

where  $\Omega_{LMP,i} = \{d_k, \dots, d_n\}$  and  $\Omega_{load,i} = \{d_l, \dots, d_m\}$  refer to the LMP cluster  $i$  and the system load cluster  $i$ , respectively;  $d_k$  is the  $k^{th}$  day in a year;  $n(\cdot)$  represents the number of elements in a set;  $\boldsymbol{\pi}_{LMP}(i, j)$  and  $\mathbf{D}_{load}(i, j)$  are the LMP and system load profiles in day  $j$  in cluster  $i$ , respectively, which represent the LMP and load for 24 hours;  $\boldsymbol{\pi}_{LMP}(i, j)$  and  $\mathbf{D}_{load}(i, j)$  are the centroids of the LMP and system load cluster  $i$ , respectively;  $p(s)$  is the discrete joint probability.

Note that each centroid is regarded as an LMP or a load profile pattern that is most likely to appear in one year.  $p(s)$

## Algorithm 1 Scenario Extraction and Reduction

Input	Historical hourly LMP and system load profiles in a year
Output	Typical LMP and system load scenarios associated with discrete joint probabilities
1)	<b>K-means clustering:</b>
2)	Utilize the elbow method to obtain the optimal number of LMP clusters and system load clusters, respectively.
3)	Partition the daily LMP and system load profiles into $k_{LMP}$ and $k_{load}$ clusters.
4)	For each cluster, calculate its centroid: $\boldsymbol{\pi}_{LMP}(i) = 1/n(\Omega_{LMP,i}) \cdot \sum_{j \in \Omega_{LMP,i}} \boldsymbol{\pi}_{LMP}(i, j)$ $\mathbf{D}_{load}(i) = 1/n(\Omega_{load,i}) \cdot \sum_{j \in \Omega_{load,i}} \mathbf{D}_{load}(i, j)$
5)	<b>Scenario generation:</b>
6)	For LMP cluster $i$ and system load cluster $j$ , calculate the discrete joint probability: $p(s) = p_{LMP,load}(i, j) = n(\Omega_{LMP,i} \cap \Omega_{load,j}) / 365$
7)	In total, $k_{LMP} \cdot k_{load}$ scenarios and corresponding probabilities are generated.
8)	<b>Scenario reduction:</b>
9)	Remove scenarios with probabilities below a threshold.
10)	Normalize the discrete joint probabilities of the remaining scenarios (let their summation be 1).

is the probability that one LMP pattern and one load pattern happen on the same day in one year. Each LMP and load pattern combination is regarded as a scenario.

### B. Variability in Nodal Loads

In the preceding subsection, the system load profile refers to the total load profile of all nodes in a distribution system. However, the load at each node is usually hard to forecast with high variability. Thus, for simplicity, it is assumed that all nodal loads have the same normalized active and reactive load profiles with the system load in each scenario [31], [32]. Additionally, a random multiplier is applied to each nodal load to simulate the randomness of the load.

$$P_{i,t}^{D,s} = \tau_{i,t}^s \cdot M_{i,t}^P \cdot P_t^{D,s} \quad (31)$$

$$Q_{i,t}^{D,s} = \tau_{i,t}^s \cdot M_{i,t}^Q \cdot Q_t^{D,s} \quad (32)$$

where  $\tau_{i,t}^s$  refers to a multiplier that follows a Gaussian distribution,  $\tau_{i,t}^s \sim N(1, 0.04^2)$ ;  $M_{i,t}^P$  and  $M_{i,t}^Q$  are the normalized active and reactive load;  $P_t^{D,s}$  and  $Q_t^{D,s}$  are the active and reactive system loads of scenario  $s$ .

## IV. SOLUTION METHODS

The previous Sections II and III build the proposed model for siting and sizing BESSs. The mathematical solution is discussed in this section.

The solution to the proposed TS-SBP model includes two steps. In the first step, the bilevel problem of the second stage is converted to a single-level problem via Karush-Kuhn Tucker (KKT) optimality conditions. After that,

the TS-SBP model becomes a two-stage stochastic MILP (TS-SMILP) problem. In the second step, based on the unique characteristics of this TS-SMILP problem, two relaxation methods are proposed to make this problem tractable.

### A. Solving the Bilevel Problem

1) *MPEC Formulation*: Due to the linear property of the lower level, its optimal solution can be obtained by solving the KKT optimality conditions [33]. Thus, the bilevel problem is converted into a single-level problem by adding the KKT conditions to the constraints of the upper level. Then the single-level problem is a mathematical program with equilibrium constraints (MPEC).

$$\max (8) \quad (33)$$

$$\text{s.t. constraints (9) – (12), (14) – (16), (22) – (24), (31) – (32)} \quad (34)$$

$$\begin{aligned} & \sigma_{i,t}^{p,s} - \lambda_t^{p,s} \left( 1 - \frac{\partial P_t^{L,s}}{\partial P_{i,t}^{G,s}} \right) - \sum_{j \in \Omega_N} (\omega_{j,t}^{v \min,s} - \omega_{j,t}^{v \max,s}) Z_{j,i}^p \\ & + \lambda_t^{q,s} \frac{\partial Q_t^{L,s}}{\partial P_{i,t}^{G,s}} - \omega_{i,t}^{p \min,s} + \omega_{i,t}^{p \max,s} = 0, \quad \forall i \in \Omega_G \end{aligned} \quad (35)$$

$$\sigma_{i,t}^{q,s} - \kappa_{i,t}^{-,s} - \kappa_{i,t}^{+,s} = 0, \quad \forall i \in \Omega_G \quad (36)$$

$$\begin{aligned} & \lambda_t^{p,s} \frac{\partial P_t^{L,s}}{\partial Q_{i,t}^{G,s}} - \lambda_t^q \left( 1 - \frac{\partial Q_t^{L,s}}{\partial Q_{i,t}^{G,s}} \right) - \sum_{j \in \Omega_N} (\omega_{j,t}^{v \min,s} - \omega_{j,t}^{v \max,s}) Z_{j,i}^q \\ & - \omega_{i,t}^{q \min,s} + \omega_{i,t}^{q \max,s} - \kappa_{i,t}^{-,s} + \kappa_{i,t}^{+,s} = 0, \quad \forall i \in \Omega_G \end{aligned} \quad (37)$$

$$0 \leq \omega_{j,t}^{v \min,s} \perp (V_{j,t}^s - V^{\min}) \geq 0, \quad \forall j \in \Omega_N \quad (38)$$

$$0 \leq \omega_{j,t}^{v \max,s} \perp (V^{\max} - V_{j,t}^s) \geq 0, \quad \forall j \in \Omega_N \quad (39)$$

$$0 \leq \omega_{i,t}^{p \min,s} \perp (P_{i,t}^{G,s} - P_i^{G,\min}) \geq 0, \quad \forall i \in \Omega_G \quad (40)$$

$$0 \leq \omega_{i,t}^{p \max,s} \perp (P_i^{G,\max} - P_{i,t}^{G,s}) \geq 0, \quad \forall i \in \Omega_G \quad (41)$$

$$0 \leq \omega_{i,t}^{q \min,s} \perp (Q_{i,t}^{G,s} - Q_i^{G,\min}) \geq 0, \quad \forall i \in \Omega_G \quad (42)$$

$$0 \leq \omega_{i,t}^{q \max,s} \perp (Q_i^{G,\max} - Q_{i,t}^{G,s}) \geq 0, \quad \forall i \in \Omega_G \quad (43)$$

$$0 \leq \kappa_{i,t}^{-,s} \perp (\bar{Q}_{i,t}^{G,s} + Q_{i,t}^{G,s}) \geq 0, \quad \forall i \in \Omega_G \quad (44)$$

$$0 \leq \kappa_{i,t}^{+,s} \perp (\bar{Q}_{i,t}^{G,s} - Q_{i,t}^{G,s}) \geq 0, \quad \forall i \in \Omega_G \quad (45)$$

where (35)-(37) are stationary conditions, and (38)-(45) are complementary slackness conditions.

2) *MILP Formulation*: The MPEC is a nonlinear problem featuring the bilinear terms found in (33) and nonlinear complementary slackness conditions. Thus, strong duality theory and the big-M method are used to reformulate the MPEC problem as a MILP problem that is tractable [33], [34].

$$\begin{aligned} & \sum_{t \in \Omega_T} \sum_{i \in \Omega_{BS}} \pi_{i,t}^s \cdot P_{i,t}^{BESS,s} \\ & = \sum_{t \in \Omega_T} \sum_{i \in \Omega_{BS}} \left( \lambda_t^{p,s} + \lambda_t^{q,s} \frac{\partial P_t^{L,s}}{\partial P_{i,t}^{G,s}} + \lambda_t^q \frac{\partial Q_t^{L,s}}{\partial P_{i,t}^{G,s}} \right. \\ & \quad \left. + \sum_{j \in \Omega_N} (\omega_{j,t}^{v \min,s} - \omega_{j,t}^{v \max,s}) Z_{j,i}^p \right) P_{i,t}^{BESS,s} \end{aligned}$$

$$\begin{aligned} & \left( \sum_{t \in \Omega_T} \lambda_t^{p,s} \left( \sum_{i \in \Omega_N} \left( 1 + \frac{\partial P_t^{L,s}}{\partial P_{i,t}^{G,s}} \right) P_{i,t}^{D,s} + \sum_{i \in \Omega_N} \frac{\partial P_t^{L,s}}{\partial Q_{i,t}^{D,s}} Q_{i,t}^{D,s} + P_t^{L0,s} \right) \right. \\ & + \sum_{t \in \Omega_T} \lambda_t^{q,s} \left( \sum_{i \in \Omega_N} \left( 1 + \frac{\partial Q_t^{L,s}}{\partial Q_{i,t}^{D,s}} \right) Q_{i,t}^{D,s} + \sum_{i \in \Omega_N} \frac{\partial Q_t^{L,s}}{\partial P_{i,t}^{D,s}} P_{i,t}^{D,s} + Q_t^{L0,s} \right) \\ & + \sum_{t \in \Omega_T} \sum_{j \in \Omega_N} \omega_{j,t}^{v \min,s} \left( V^{\min} - V_{sub,t}^s + \sum_{i \in \Omega_N} Z_{j,i}^p P_{i,t}^{D,s} + \sum_{i \in \Omega_N} Z_{j,i}^q Q_{i,t}^{D,s} \right) \\ & - \sum_{t \in \Omega_T} \sum_{j \in \Omega_N} \omega_{j,t}^{v \max,s} \left( V^{\max} - V_{sub,t}^s + \sum_{i \in \Omega_N} Z_{j,i}^p P_{i,t}^{D,s} + \sum_{i \in \Omega_N} Z_{j,i}^q Q_{i,t}^{D,s} \right) \\ & + \sum_{t \in \Omega_T} \sum_{i \in \Omega_G} (\omega_{i,t}^{p \min,s} P_i^{G,\min} - \omega_{i,t}^{p \max,s} P_i^{G,\max}) \\ & + \sum_{t \in \Omega_T} \sum_{i \in \Omega_G} (\omega_{i,t}^{q \min,s} Q_i^{G,\min} - \omega_{i,t}^{q \max,s} Q_i^{G,\max}) \\ & \left. - \sum_{t \in \Omega_T} \left( \sigma_{sub,t}^{p,s} P_{sub,t}^{G,s} + \sigma_{sub,t}^{q,s} \bar{Q}_{sub,t}^{G,s} + \sum_{i \in \Omega_G} (\sigma_{i,t}^{p,s} P_{i,t}^{G,s} + \sigma_{i,t}^{q,s} \bar{Q}_{i,t}^{G,s}) \right) \right) \end{aligned} \quad (46)$$

The objective function (33) is reformulated as (46). Each constraint in (38)-(45) is reformulated as:

$$0 \leq \omega_{i,t} \leq M_{i,t} v_{i,t}, \quad 0 \leq g_{i,t}(x) \leq M_{i,t}(1 - v_{i,t}) \quad (47)$$

So far, the completed MILP problem can be presented as follows:

$$\max (46) \quad (48)$$

$$\text{s.t. constraints (34)–(37), (47).} \quad (49)$$

### B. Solving the Two-Stage Problem

With the reformulation of the second stage in the preceding subsection, the TS-SBP problem becomes a TS-SMILP problem which is a large-scale optimization problem that requires huge computational resources. To reduce the computational burden, the problem scale can be reduced via two aspects according to the specific characteristics of the original problem.

1) *Candidate BESS Buses Reduction*: The candidate BESS buses are binary variables that are associated with a series of constraints. However, only a limited number of buses are realistic candidate sites for BESSs due to geographical, physical, and spatial limits in industrial practices. Thus, these candidate buses can be reduced to a limited set of probable buses instead of all buses.

2) *Inactive Voltage Constraints Reduction*: Continuous and binary variables, especially voltage-related ones in the second stage, account for most of the constraints and decision variables throughout the entire problem. However, most voltage constraints are inactive, and they can be omitted to reduce the number of complementary slackness conditions.

The complete solution procedure including detailed candidate buses and inactive voltage constraints reduction is described in Algorithm 2.

It should be noted that step 3 is more like data pre-processing, since candidate buses may be influenced by the investor's preference as well as the actual operating conditions which are hard to handle quantitatively. Here, step 3 obtains the most probable installation buses, but does not ensure equivalence with the original problem.

### Algorithm 2 Overall Solution Procedure

**1. Decomposition:** Since there is a finite set of scenarios, (25) can be reformulated as:

$$\max_{s \in \mathcal{S}} 365 \cdot \sum_{s \in \mathcal{S}} p(s) \left( -c^T x_s + \pi_s^T y_s \right)$$

Decompose it into  $S$  subproblems.

**2. Initialization:** For each  $s \in \mathcal{S}$ , compute:

$$(x_s, y_s) \in \arg \max -c^T x_s + \pi_s^T y_s$$

**3. Candidate buses reduction:** Obtain the aggregated binary variable:  $\hat{\delta} = \sum_{s \in \mathcal{S}} p_s(s) \delta_s$ , where  $\hat{\delta} = \{\hat{\delta}_1, \dots, \hat{\delta}_{\Omega_N}\}$ ; remove  $\hat{\delta}_i$

with low values; the rest are the most probable buses.

**4. Voltage constraints reduction:** Check  $V_s = \{V_1, \dots, V_{\Omega_N}\}$ ,  $s \in \mathcal{S}$ , identify buses at which at which voltage constraints are never violated; then, remove constraints at these buses.

**5. Solving:** With reduced candidate buses and voltage constraints, compute:  $(x, y_s) \in \arg \max -c^T x + 365 \cdot \sum_{s \in \mathcal{S}} p(s) \pi_s^T y_s$ .

**6. Voltage constraints update:** Check whether the removed voltage constraints are violated or not. If yes, add the violated ones and go back to **Step 5**; otherwise, the algorithm terminates.

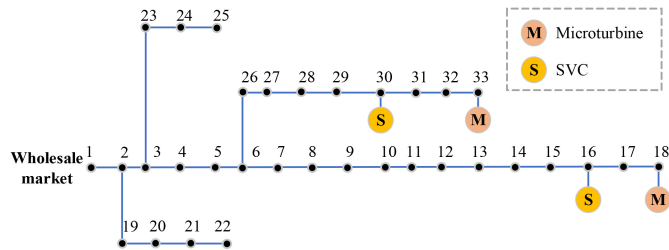


Fig. 2. Modified IEEE 33-bus system.

## V. CASE STUDIES

The proposed model is tested on the modified IEEE 33-bus and 123-bus distribution systems. Simulations are performed on a personal laptop with an Intel Core i7-8650U CPU and 16GB RAM. The codes are carried out in MATLAB R2020a, YALMIP and GUROBI 9.0.0.

### A. IEEE 33-Bus Distribution System

1) *System Description:* The modified IEEE 33-bus system is illustrated in Fig. 2. Two MTs are located at buses 18 and 33, respectively, and two SVCs are located at buses 16 and 30, respectively. The parameters of DGs, the distribution system, BESS investment and operating constraints are listed in Table I.

2) *Scenario Extraction:* The daily day-ahead LMP and load profiles in one year have been obtained from PJM [35], and the time range is 1/1/2020-12/31/2020. After  $k$ -means clustering, the optimal cluster numbers obtained via the elbow method are  $k_{LMP} = 7$  and  $k_{load} = 6$ , respectively. The normalized LMP patterns, load patterns, and their discrete joint probabilities are shown in Fig. 3. It can be seen that some probabilities are 0 which means the corresponding LMP pattern and load pattern have never appeared on the same day. Thus, among the 42 scenarios, we can remove the scenarios with probabilities less than 0.01. Then, 21 scenarios are kept.

TABLE I  
PARAMETERS OF THE MODIFIED IEEE 33-BUS SYSTEM

Class	Parameter	Typical Value
MT	Location	Bus #18, 33
	Bidding price	\$ 70/MWh
	Capacity	0.5 MW
	$\alpha_i$	0.95
SVC	Location	Bus #16, 30
	Bidding price	\$ 0/MVarh
	Capacity	0.5 MVar
System constraints	$V^{min}$	0.95 p.u.
	$V^{max}$	1.05 p.u.
	$V_{sub}$	1.0 p.u.
	Peak load	6.316 MW + $j$ 3.026 MVar
Investment constraints	$N_{BS}^{max}$	5
	$C^{Bgt}$	\$ $1 \times 10^6$
	$P^{min} / P^{max}$	0.1 MW / 0.4 MW
	$E^{min} / E^{max}$	0.4 MWh / 1.2 MWh
BESS operating constraints	$SOC_i^{min} / SOC_i^{max}$	0.2 / 0.8
	$\eta_i$	0.81

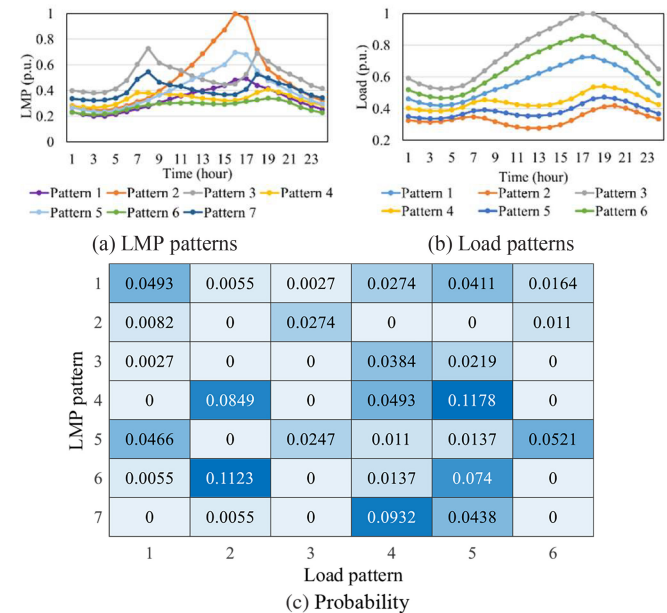


Fig. 3. LMP patterns, load patterns, and their discrete joint probabilities.

The best method for validating the effect of the scenario extraction is comparing the optimal sites and sizes by solving the proposed TS-SBP model with both 365 scenarios (1-year LMP and load data) and only the extracted scenarios, respectively. However, solving the proposed TS-SBP model with a full 365 scenarios requires huge computational resources, and is therefore unmanageable in our current laboratory environment. Thus, an alternative method is proposed to achieve the validation: given the optimal sites and sizes obtained by the extracted scenarios, we compare the annual net profit of all 365 scenarios with the annual net profit of the extracted scenarios. Due to the variability consideration of nodal loads in (31)(32), the simulation is run multiple times.

The average annual net profit curves are illustrated in Fig. 4, which shows that the curves in the two cases become flat and

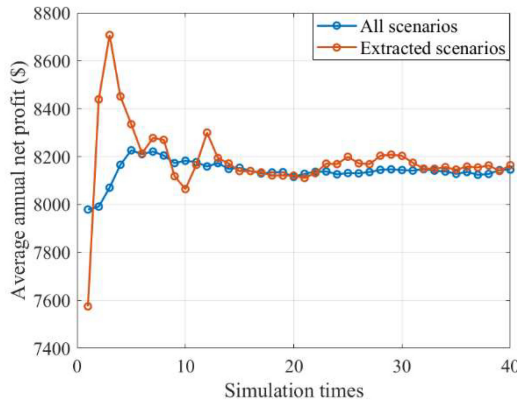


Fig. 4. Average annual net profit of all scenarios and that of extracted scenarios.

TABLE II  
DIFFERENT CASES

Cases	Reduced Items		
	Scenarios	Voltage constraints	Candidate buses
Case 1	×	×	×
Case 2	√	×	×
Case 3	√	×	√
Case 4	√	√	×
Case 5	√	√	√

\*×: not reduced, √: reduced.

closer as the simulation time increases. Beyond the 32<sup>nd</sup> simulation, the profits of all 365 scenarios (\$8124.02-\$8147.70), and the profits of only the extracted scenarios (\$8140.08-\$8164.32) both stay within a tight range. This comparison demonstrates that given the BESS allocations, the expected annual profit obtained by the extracted scenarios can be very close to that of all 365 scenarios, which validates the effectiveness of the scenario extraction strategy.

3) *BESS Siting and Sizing Results*: After Algorithm 2 has been performed, 11 buses are selected as the most probable BESS candidate buses,  $\Omega_{BS} = \{10-12, 14-18, 31-33\}$ , the voltage constraints at 12 buses are kept,  $\Omega_V = \{9-15, 17-18, 31-33\}$ .

To verify the effectiveness of the proposed scale reduction methods, five cases with different reduced items are formulated in Table II. Table III presents the siting and sizing results.

Table III shows that Cases 1-5 have the same BESS siting and sizing results. The annual net profit of Case 1 is slightly different, which is reasonable because Case 1 considers more scenarios. Cases 2-5 have close annual net profits, but significantly different computational times. In these cases, both candidate bus reduction and inactive voltage constraint reduction improve computational efficiency. Their combination makes for the best-observed performance.

A comparison of intermediate results among Cases 2-5 is presented since Cases 2-5 are all simulated using the same reduced number of scenarios. Here, Case 2 is set as the benchmark and Cases 3-5 are compared with Case 2. The number of constraints and variables, the accumulated difference of voltage, the DLMP, DG power output, and BESS power output are provided in Table IV. The accumulated voltage difference is calculated using the following

TABLE III  
RESULTS OF DIFFERENT CASES BASED ON THE IEEE 33-BUS SYSTEM

Cases	BESS bus (#)	$P^{rated} / E^{rated}$ (kW/ kWh)	Annual net profit (\$)	Time (s)
Case 1	11, 15, 18, 31, 33	100/400, 149/597, 103/414, 107/426, 100/400	9302.22	7936
Case 2	11, 15, 18, 31, 33	100/400, 149/597, 103/414, 107/426, 100/400	9129.37	3442
Case 3	11, 15, 18, 31, 33	100/400, 149/597, 103/414, 107/426, 100/400	9129.38	1338
Case 4	11, 15, 18, 31, 33	100/400, 149/597, 103/414, 107/426, 100/400	9129.38	2390
Case 5	11, 15, 18, 31, 33	100/400, 149/597, 103/414, 107/426, 100/400	9129.38	1077

TABLE IV  
COMPARISON OF INTERMEDIATE RESULTS FROM THE IEEE 33-BUS SYSTEM

Cases	Constraint	Variable	$\Delta V$	$\Delta DLMP$	$\Delta P^{DG}$	$\Delta P^{BESS}$
Case 2	410801	227907	--	--	--	--
Case 3	321063	183489	0.0162	0.0938	0.0317	0.4189
Case 4	326129	185571	0.0162	0.0938	0.0317	0.4189
Case 5	236391	141153	0.0162	0.0938	0.0317	0.4189

equation:

$$\Delta V = \sum_{s \in S} \sum_{t \in \Omega_T} \sum_{j \in \Omega_N} \frac{|V_{j,t}^{s,rel} - V_{j,t}^{s,ben}|}{V^{ben,max}} \quad (50)$$

where  $V_{j,t}^{s,rel}$  and  $V_{j,t}^{s,ben}$  are the voltage of scenario  $s$  at bus  $j$  and time  $t$  for the relaxed case and benchmark case respectively, and  $V^{ben,max}$  is the maximum value. The DLMP difference ( $\Delta DLMP$ ), DG power output difference ( $\Delta P^{DG}$ ), and BESS power output difference ( $\Delta P^{BESS}$ ) are calculated using a similar formula. Note that the accumulated difference is the summation of individual differences across all scenarios at all time slots and all buses.

From Table IV, it can be found that the application of relaxations reduces the number of constraints and decision variables, and all of the accumulated differences are small in value. All of these cases validate the effectiveness of the proposed scale reduction methods.

The expected DLMP is defined as the weighted sum of the DLMPs of all scenarios. It is illustrated in Fig. 5. The optimal BESS locations are buses #11, 15, 18, 31, and 33. These locations are intuitively reasonable because the daily DLMP gap (the difference between the highest DLMP and the lowest DLMP) is high in these buses, as shown in Fig. 5. Therefore, BESS owners make a higher profit. It can be concluded that the DLMP provides effective market signals for BESS investment. On the other hand, the higher DLMP reflects the scarcity of generation resources and stressed operating conditions. Thus, from the perspective of the DSO, installing BESSs in these locations will increase the local power supply, and benefit the stressed distribution system with a positive effect for the DSO.



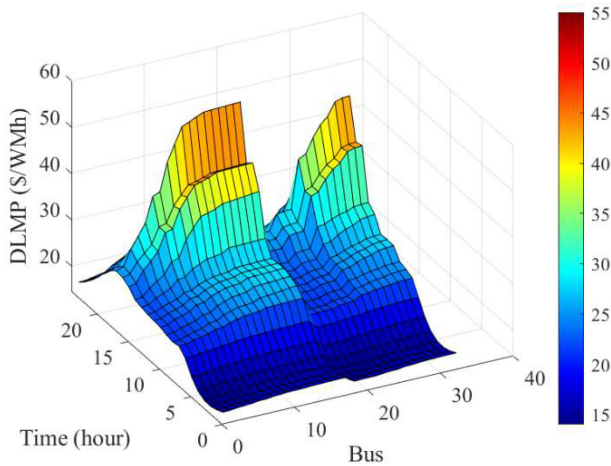


Fig. 5. Expected DLMP.

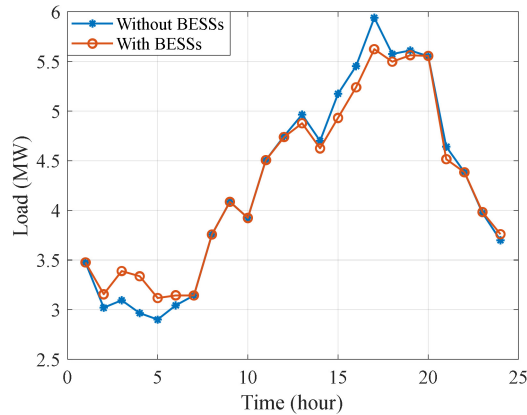


Fig. 6. System load profiles with and without BESSs in the IEEE 33-Bus system.

This is aligned with the incentive compatibility mechanism. System improvement is discussed in the next subsection.

4) *Load Profile and Voltage Improvement*: Among the reduced scenarios, we select scenario 13 which has the highest system load level. In the second stage, system load profiles over one day before and after BESS installation are shown in Fig. 6. It can be found that with the integration of BESSs, peak load at  $t = 13:00-19:00$  is shifted to off-peak hours  $t = 2:00-6:00$ . The operation stress under heavy load conditions is relieved.

The nodal voltage profiles in this scenario after BESS installation are shown in Fig. 7. It can be observed that the voltage profiles over one day are well maintained within the voltage boundaries.

5) *Effect of DERs Penetration Level*: With the integration of various DERs, the number of existing DERs can also affect the optimal allocation of BESSs. In this subsection, four cases are formulated to study the effects of different DERs penetration levels. Here, photovoltaics (PVs) are selected as a new DER with a bidding price of \$15/MWh and a capacity of 0.5 MW. The locations of DERs are listed in Table V. The simulation results can be found in Table VI.

From Table VI, it can be seen that with an increasing level of DERs penetration, the optimal BESS allocation is changed and

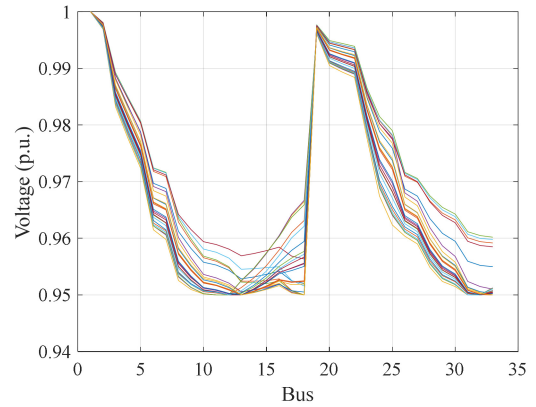


Fig. 7. Nodal voltage profiles with BESSs in the IEEE 33-bus system.

TABLE V  
DIFFERENT DERs PENETRATION LEVELS

Cases	DERs	Amount	Bus (#)
Case 1	SVC	2	16, 30
	MT	2	18, 33
	PV	0	None
Case 2	SVC	2	16, 30
	MT	2	18, 33
	PV	2	12, 28
Case 3	SVC	2	16, 30
	MT	3	8, 18, 33
	PV	3	12, 14, 28
Case 4	SVC	3	10, 16, 30
	MT	4	8, 18, 26, 33
	PV	5	12, 14, 17, 31, 32

TABLE VI  
RESULTS OF DIFFERENT DER PENETRATION LEVELS

Cases	BESS bus (#)	$P^{rated} / E^{rated}$ (kW/kWh)	Annual net profit (\$)	Time (s)
Case 1	11, 15, 18, 31, 33	100/400, 149/597, 103/414, 107/426, 100/400	9129.37	1077
Case 2	15, 18, 32, 33	100/400, 149/597, 100/400, 210/840	5858.96	492
Case 3	16, 18, 32, 33	101/405, 141/563, 100/400, 217/869	5705.55	580
Case 4	16, 18, 32, 33	100/400, 129/514, 100/400, 231/923	5184.61	1692

the annual net profit is reduced. The main reason is as follows: Compared to MTs and the wholesale LMP, PVs usually have the lowest bidding price, thus they easily win the bidding. With the large-scale integration of PVs, the DLMP profile changes and the overall system DLMP is reduced. Since the optimal allocation of BESSs is closely related to the DLMP, the allocation and profit are changed as well. A more comprehensive analysis of profit reduction can be found in [34].

PVs are studied here because they are one of the most common DGs that can be installed in the distribution system. PVs can be replaced by other DGs and the simulation results will be different, but the in-depth reasoning should be similar. Also note, BESS mitigation of the volatility of PVs is not the focus of this paper.

TABLE VII  
COMPARISON WITH OTHER MODELS BASED ON THE IEEE  
33-BUS SYSTEM

Models	BESS bus (#)	$P^{rated}/E^{rated}$ (kW/kWh)	Annual net profit (\$)
Proposed model	11, 15, 18, 31, 33	100/400, 149/597, 103/414, 107/426, 100/400	9129.37
Model 2	11, 15, 17, 32, 33	112/448, 112/448, 112/448, 111/445, 112/448	8780.28
Model 3	11, 15, 16, 18, 33	100/400, 110/439, 100/400, 103/413, 146/585	8794.21

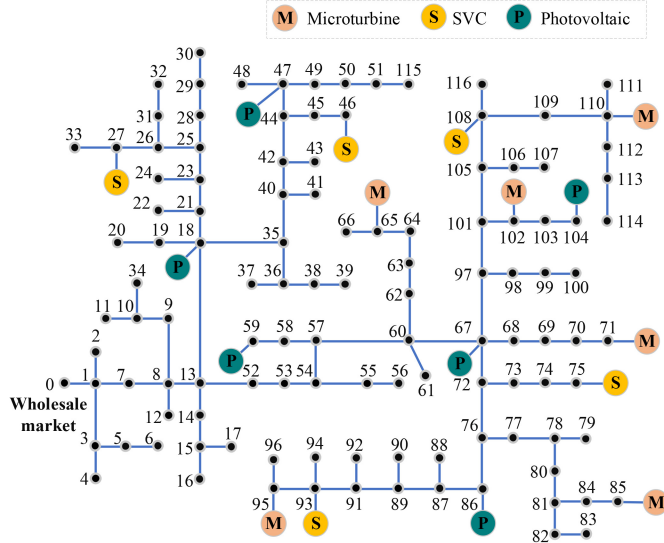


Fig. 8. Modified IEEE 123-bus system.

6) *Comparison With Other Models:* To demonstrate the advantage of the proposed model, the optimal BESS allocation of our proposed model is compared with two other models. The formulation of these two comparative models are elaborated next. In Model 2, it is assumed that all BESSs have the same fixed sizes and only the BESS sites are to be determined. In Model 3, the candidate bus set is  $\Omega_{BS} = \{11-18, 33\}$ , which is obtained by the method proposed in [22], and other conditions are kept the same as in our proposed model. The simulation results are shown in Table VII. The BESS locations in Model 2 are close to the BESS locations of the proposed model, but the annual net profit is suboptimal. In Model 3, the candidate bus set determination and optimal siting and sizing are separated, and its profit is not the best. This indicates that a comprehensive algorithm (e.g., Algorithm 2) that combines these two items is truly effective and promising.

## B. IEEE 123-Bus Distribution System

1) *System Description:* The topology of the modified IEEE 123-bus system is shown in Fig. 8. Six MTs, five SVCs and six PVs are already installed in the system. Parameters of the system are listed in Table VIII. System constraints, BESS investment, and operating constraints are the same as those in Table I.

2) *BESS Siting and Sizing Results:* The normalized LMP patterns, load patterns, and their discrete joint probabilities are the same as those in Fig. 3. To reduce the computational

TABLE VIII  
PARAMETERS OF THE MODIFIED IEEE 123-BUS SYSTEM

Class	Parameter	Typical Value
MT	Location	Bus #65, 71, 85, 95, 102, 110
	Bidding price	\$ 70/MWh
	Capacity	0.5 MW
	$\alpha_i$	0.95
SVC	Location	Bus #27, 46, 75, 93, 108
	Bidding price	\$ 0/MVarh
	Capacity	0.5 MVar
PV	Location	Bus #18, 47, 59, 67, 86, 104
	Bidding price	\$ 15/MWh
	Capacity	0.5 MW
	$\alpha_i$	0.95
System parameters	Peak load	7.06 MW + j3.88 MVar

TABLE IX  
RESULTS OF DIFFERENT CASES BASED ON THE IEEE 123-BUS SYSTEM

Cases	BESS bus (#)	$P^{rated}/E^{rated}$ (kW/kWh)	Annual net profit (\$)	Time (s)
Case 1	N/A	N/A	N/A	N/A
Case 2	65, 66, 85, 113	100/400, 159/635, 200/802, 100/400	4604.90	9808
Case 3	65, 66, 85, 114	100/400, 160/642, 199/795, 100/400	4604.30	2790
Case 4	65, 66, 85, 113	100/400, 159/635, 200/802, 100/400	4604.90	2126
Case 5	65, 66, 85, 114	100/400, 160/642, 199/795, 100/400	4604.30	1272

TABLE X  
COMPARISON OF INTERMEDIATE RESULTS FROM THE IEEE  
123-BUS SYSTEM

Cases	Constraint	Variable	$\Delta V$	$\Delta DLMP$	$\Delta p^{DG}$	$\Delta p^{BESS}$
Case 2	100426	554079	--	--	--	--
Case 3	662277	384789	0.1175	0.0456	0.0615	1.2686
Case 4	709355	406623	9.3e-9	9.4e-10	2.3e-8	9.3e-9
Case 5	367365	237333	0.1175	0.0456	0.0615	1.2686

burden, scenarios with probabilities less than 0.02 were removed. Then, 16 scenarios have been kept.

After Algorithm 2 is performed, seven buses are selected as the candidate BESS buses,  $\Omega_{BS} = \{65, 66, 85, 94, 104, 112, 114\}$ , while the voltage constraints at twenty buses are kept,  $\Omega_V = \{65, 66, 71, 75, 83-85, 87-96, 104, 113, 114\}$ . Table IX and Table X present the simulation results of the five cases that are formulated in Table II. Table IX shows that the sites and sizes of Cases 2 & 4 and Cases 3 & 5 are slightly different. This validates the discussion at the end of Section IV that the reduction of candidate buses does not ensure equivalence with the original problem. However, these results are still very close; the cases all have similar annual net profit, similar sizes, and similar BESS locations. Thus, the allocation results of Case 5 are acceptable for investors.

Table X shows that all of the accumulated differences between Cases 2-5 are still small in value. Comparing the number of constraints and variables in Table X with that in Table IV, we can observe that a greater portion of the constraints and variables have been eliminated. This indicates that these relaxation strategies perform better as the system scale increases. The computational time is maintained at an

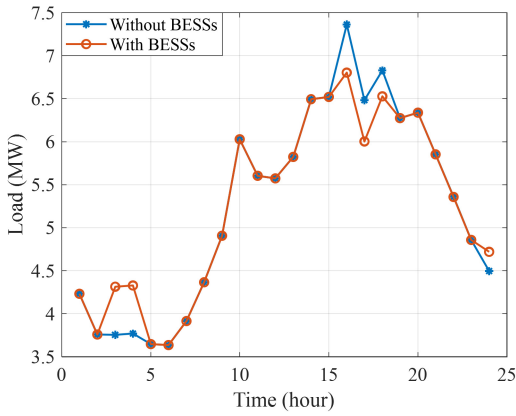


Fig. 9. System load profiles with and without BESSs in the IEEE 123-Bus system.

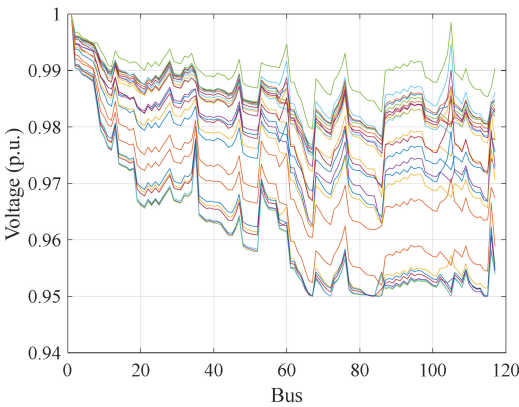


Fig. 10. Nodal voltage profiles with BESSs in the IEEE 123-Bus system.

TABLE XI  
COMPARISON WITH OTHER MODELS BASED ON THE IEEE  
123-BUS SYSTEM

Models	BESS bus (#)	$P^{rated} / E^{rated}$ (kW/ kWh)	Annual net profit (\$)
Proposed model	65, 66, 85, 114	100/400, 160/642, 199/795, 100/400	4604.30
Model 2	65, 66, 85, 114	140/560, 140/560, 140/560, 139/557	4589.28
Model 3	66, 85, 113	256/1023, 203/814, 100/400	4601.14

acceptable level, further demonstrating that the proposed relaxation strategies can achieve a tradeoff between accuracy and efficiency.

3) *Load Profile and Voltage Improvement of BESS*: In this subsection, scenario 4 is selected. Fig. 9 shows the load shifting effect, as the load at  $t = 16:00-18:00$  is shifted to off-peak hours  $t = 3:00-4:00$ . The nodal voltage profiles with BESSs are shown in Fig. 10, and the voltage profiles are well maintained.

4) *Comparison With Other Models*: A comparison of our proposed model with other models is presented in Table XI. In Model 3, the candidate bus set is  $\Omega_{BS} = \{66, 71, 75, 84, 85, 104, 111-114\}$ . It can be found that Model 2 and the proposed model have the same optimal BESS sites, but Model 2's profit is not the best. In Model 3, the number of optimal BESS

sites is reduced to just 3. This further shows that the joint optimization of sites and sizes is the best choice for the profit-oriented BESS planning problem.

## VI. CONCLUSION

In this paper, a profit-oriented BESS planning problem that sites and sizes BESSs, is proposed in a deregulated distribution system with the integration of the DLMP. This problem is formulated as a TS-SBP model, in which the first stage determines the optimal sites and sizes of BESSs, and the second stage maximizes investors' operating revenue. Typical operating scenarios are extracted from a historical dataset by statistical methods. Two scale-reduction strategies are proposed to relax the original problem. Numerical studies on two systems illustrate the following conclusions:

1) The DLMP can act as an effective price signal to incentivize BESS planning. This is a special attribute of the deregulated system that is quite different from traditional systems.

2) The two proposed scale-reduction strategies are verified to both significantly improve computational efficiency and maintain result accuracy.

3) Optimal siting and sizing are shown to be beneficial for both BESS investors and the DSO, such that our proposed model is aligned with incentive compatibility in market operation.

Although only the energy market is studied in this paper, BESSs can also participate in the ancillary service market to mitigate the uncertainty of renewable generators or regulate system frequency, topics which we may explore in future works. Additionally, the proposed model and solution methods can be easily extended to other DER planning problems. Future work may also be extended to resilience-oriented BESS planning for areas where resilience or extreme weather events are a major concern.

## APPENDIX A COST OF LFP BATTERIES

According to [27], BESS costs mainly consist of capital and operation costs. The capital cost refers to the BESS installation cost which includes power-related costs and energy-related costs. The former consists of power equipment costs (costs of the converter, protection, breaker, communication, software, etc.), controls & communication costs (cost of the energy management system for the BESS), and grid integration costs (cost of integrating the BESS to the power system, including transformers and isolation breakers).

The energy-related costs consist of storage block costs (cost of the storage elements in a BESS), storage balance of system costs (cost of supporting components like containers, cabling, switchgears, flow battery pumps, and HVAC), system integration costs (costs of integrating subcomponents of a BESS into a functional system), and project development costs (costs of permitting, power purchase agreements, etc.).

Operation costs include the fixed and variable costs for O&M. The fixed O&M cost refers to the costs necessary to keep the BESS operational, such as planned maintenance.

TABLE A1  
COST OF LFP BATTERIES

$k^p$ (\$/kW)	156
$k^e$ (\$/kWh)	408
$c^{Mf}$ (\$/kW-yr)	4.4
$c^{Mv}$ (\$/kWh)	0.5125e-3

TABLE A2  
DIFFERENCES BETWEEN BESSs AND MESSs

Features	BESSs	MESSs
Investment cost	Expensive	Very expensive
Operation style	Stationary	Transportable
Moving time	No	Yes
Transportation cost	No	Yes
Localized services	Good	Excellent

The variable O&M cost represents the usage impacted cost necessary to operate the storage system.

BESS costs are summarized in Table A1. In this paper, all BESSs are lithium-ion iron phosphate (LFP) batteries due to their good safety performance and long lifespan. For more details, [36], [37] have presented a detailed analysis and comparison of different types of batteries.

## APPENDIX B

### COMPARISON BETWEEN BESSs AND MESSs

In addition to BESSs, mobile energy storage systems (MESSs) are another promising storage technology [38]. BESSs and MESSs share many similar functions such as load shifting, peak shaving, reactive power support, renewable energy integration, transmission deferral, energy arbitrage, and voltage profile improvement. The general operational and economic differences between BESSs and MESSs are summarized in Table A2. It can be concluded that the main advantage of a BESS is its lower cost (e.g., investment plus transportation), while the main advantage of a MESS is its better location-based services (e.g., voltage regulation and power loss minimization) due to its locational flexibility. In a competitive distribution system, it may be difficult to claim that BESSs will always be more attractive than MESSs, or vice versa. Thus, the preliminary conclusion regarding the decision of whether to invest in BESSs or MESSs really depends on the requirements and preferences of the investors and the features of the distribution system. A more rigorous study should be conducted for a given system to make the best decision.

## REFERENCES

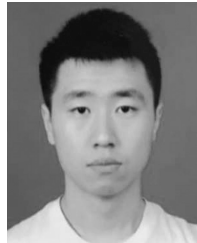
- [1] J. J. Cook, K. Ardani, E. O'Shaughnessy, B. Smith, and R. Margolis, "Expanding PV value: Lessons learned from utility-led distributed energy resource aggregation in the United States," NREL, Denver, CO, USA, Rep. NREL/TP-6A20-71984, Nov. 2018.
- [2] H. Yuan, F. Li, Y. Wei, and J. Zhu, "Novel linearized power flow and linearized OPF models for active distribution networks with application in distribution LMP," *IEEE Trans. Smart Grid*, vol. 9, no. 1, pp. 438–448, Jan. 2018.
- [3] L. Bai, J. Wang, C. Wang, C. Chen, and F. Li, "Distribution locational marginal pricing (DLMP) for congestion management and voltage support," *IEEE Trans. Power Syst.*, vol. 33, no. 4, pp. 4061–4073, Jul. 2018.

- [4] R. Li, Q. Wu, and S. S. Oren, "Distribution locational marginal pricing for optimal electric vehicle charging management," *IEEE Trans. Power Syst.*, vol. 29, no. 1, pp. 203–211, Jan. 2014.
- [5] W. Liu, Q. Wu, F. Wen, and J. Østergaard, "Day-ahead congestion management in distribution systems through household demand response and distribution congestion prices," *IEEE Trans. Smart Grid*, vol. 5, no. 6, pp. 2739–2747, Jul. 2014.
- [6] Y. Wu, M. Barati, and G. J. Lim, "A pool strategy of microgrid in power distribution electricity market," *IEEE Trans. Power Syst.*, vol. 35, no. 1, pp. 3–12, Jan. 2020.
- [7] B. S. K. Patnam and N. M. Pindoriya, "DLMP calculation and congestion minimization with EV aggregator loading in a distribution network using bilevel program," *IEEE Syst. J.*, vol. 15, no. 2, pp. 1835–1846, Jun. 2021.
- [8] Federal Energy Regulatory Commission (FERC), Order No. 755, "Frequency Regulation Compensation in the Organized Wholesale Power Markets," Oct. 2011. [Online]. Available: <https://www.ferc.gov/sites/default/files/2020-06/OrderNo.755.pdf>
- [9] Federal Energy Regulatory Commission (FERC), Order No. 841, "Electric Storage Participation in Markets Operated by Regional Transmission Organizations and Independent System Operators," Feb. 2018. [Online]. Available: <https://www.ferc.gov/media/order-no-841>
- [10] Federal Energy Regulatory Commission (FERC), Order No. 2222, "A New Day For Distributed Energy Resources," Sep. 2020. [Online]. Available: <https://www.ferc.gov/media/ferc-order-no-2222-fact-sheet>
- [11] L. Xu and D. Tretheway, *Flexible Ramping Products*, California Independent Syst. Oper., Folsom, CA, USA, 2012.
- [12] H. Chen, S. Baker, S. Benner, A. Berner, and J. Liu, "PJM integrates energy storage: Their technologies and wholesale products," *IEEE Power Energy Mag.*, vol. 15, no. 5, pp. 59–67, Sep./Oct. 2017.
- [13] *Battery Storage in the United States: An Update on Market Trends*, U.S. Energy Inf. Admin., Washington, DC, USA, Jul. 2020.
- [14] R. Fernández-Blanco, Y. Dvorkin, B. Xu, Y. Wang, and D. S. Kirschen, "Optimal energy storage siting and sizing: A WECC case study," *IEEE Trans. Sustain. Energy*, vol. 8, no. 2, pp. 733–743, Apr. 2017.
- [15] Y. Tang and S. H. Low, "Optimal placement of energy storage in distribution networks," *IEEE Trans. Smart Grid*, vol. 8, no. 6, pp. 3094–3103, Nov. 2017.
- [16] L. Bai, T. Jiang, F. Li, H. Chen, and X. Li, "Distributed energy storage planning in soft open point based active distribution networks incorporating network reconfiguration and DG reactive power capability," *Appl. Energy*, vol. 210, pp. 1082–1091, Jan. 2018.
- [17] M. R. Jannesar, A. Sedighi, M. Savaghebi, and J. M. Guerrero, "Optimal placement, sizing, and daily charge/discharge of battery energy storage in low voltage distribution network with high photovoltaic penetration," *Appl. Energy*, vol. 226, pp. 957–966, Sep. 2018.
- [18] X. Su *et al.*, "Sequential and comprehensive BESSs placement in unbalanced active distribution networks considering the impacts of BESS dual attributes on sensitivity," *IEEE Trans. Power Syst.*, vol. 36, no. 4, pp. 3453–3464, Jul. 2021.
- [19] W. Wei, D. Wu, Z. Wang, S. Mei, and J. P. S. Catalão, "Impact of energy storage on economic dispatch of distribution systems: A multi-parametric linear programming approach and its implications," *IEEE Open Access J. Power Energy*, vol. 7, pp. 243–253, 2020.
- [20] S. A. Rafiei, B. Mohammadi-Ivatloo, S. Asadi, S. Goldani, and H. Falaghi, "Bi-level model for generation expansion planning with contract pricing of renewable energy in the presence of energy storage," *IET Renew. Power Gener.*, vol. 13, no. 9, pp. 1544–1553, 2019.
- [21] X. Xiao, F. Wang, M. Shahidehpour, Z. Li, and M. Yan, "Coordination of distribution network reinforcement and DER planning in competitive market," *IEEE Trans. Smart Grid*, vol. 12, no. 3, pp. 2261–2271, May 2021.
- [22] M. H. S. Boloukat and A. A. Foroud, "Multi-period planning of distribution networks under competitive electricity market with penetration of several microgrids, part I: Modeling and solution methodology," *IEEE Trans. Ind. Informat.*, vol. 14, no. 11, pp. 4884–4894, Nov. 2018.
- [23] R. Atia and N. Yamada, "Distributed renewable generation and storage systems sizing in deregulated energy markets," in *Proc. Int. Conf. Renew. Energy Res. Appl. (ICRERA)*, Palermo, Italy, Nov. 2015, pp. 258–262.
- [24] E. Samani and F. Aminifar, "Tri-level robust investment planning of DERs in distribution networks with AC constraints," *IEEE Trans. Power Syst.*, vol. 34, no. 5, pp. 3749–3757, Sep. 2019.
- [25] P. Lamaina, D. Sarno, P. Siano, A. Zakariazadeh, and R. Romano, "A model for wind turbines placement within a distribution network acquisition market," *IEEE Trans. Ind. Informat.*, vol. 11, no. 1, pp. 210–219, Feb. 2015.

- [26] R. E. Brown and M. Marshall, "Budget constrained planning to optimize power system reliability," *IEEE Trans. Power Syst.*, vol. 15, no. 2, pp. 887–892, May 2000.
- [27] K. Mongird, V. Viswanathan, J. Alam, C. Vartanian, V. Sprenkle, and R. Baxter, "2020 Grid energy storage technology cost and performance assessment," United States Dept. Energy, Pac. Northwest Nat. Lab., Richland, WA, USA, Rep. DOE/PA-0204, Dec. 2020.
- [28] C. Opathella, A. Elkasrawy, A. A. Mohamed, and B. Venkatesh, "Optimal scheduling of merchant-owned energy storage systems with multiple ancillary services," *IEEE Open Access J. Power Energy*, vol. 7, pp. 31–40, 2020.
- [29] H. Cui, F. Li, X. Fang, H. Chen, and H. Wang, "Bilevel arbitrage potential evaluation for grid-scale energy storage considering wind power and LMP smoothing effect," *IEEE Trans. Sustain. Energy*, vol. 9, no. 2, pp. 707–718, Apr. 2018.
- [30] Q. Shi *et al.*, "Network reconfiguration and distributed energy resource scheduling for improved distribution system resilience," *Int. J. Electr. Power Energy Syst.*, vol. 124, pp. 1–10, Jan. 2021.
- [31] S. Ma, L. Su, Z. Wang, F. Qiu, and G. Guo, "Resilience enhancement of distribution grids against extreme weather events," *IEEE Trans. Power Syst.*, vol. 33, no. 5, pp. 4842–4853, Sep. 2018.
- [32] Q. Shi *et al.*, "Resilience-oriented DG siting and sizing considering stochastic scenario reduction," *IEEE Trans. Power Syst.*, vol. 36, no. 4, pp. 3715–3727, Jul. 2021.
- [33] A. J. Conejo and C. Ruiz, "Complementarity, not optimization, is the language of markets," *IEEE Open Access J. Power Energy*, vol. 7, pp. 344–353, 2020.
- [34] X. Wang *et al.*, "Tri-level scheduling model considering residential demand flexibility of aggregated HVACs and EVs under distribution LMP," *IEEE Trans. Smart Grid*, vol. 12, no. 5, pp. 3990–4002, Sep. 2021.
- [35] (PJM, Audubon, PA, USA). *Data Miner 2*. Accessed: May 20, 2021. [Online]. Available: <http://dataminer2.pjm.com/list>
- [36] A. Dinger, R. Martin, X. Mosquet, D. Rizoulis, M. Russo, and G. Sticher, *Batteries for Electric Cars: Challenges, Opportunities, and the Outlook to 2020*, Boston Consulting Group, Boston, MA, USA, 2010.
- [37] M. Stecca, L. R. Elizondo, T. B. Soeiro, P. Bauer, and P. Palensky, "A comprehensive review of the integration of battery energy storage systems into distribution networks," *IEEE Open J. Ind. Electron. Soc.*, vol. 1, pp. 46–65, 2020.
- [38] H. H. Abdeltawab and Y. A.-R. I. Mohamed, "Mobile energy storage scheduling and operation in active distribution systems," *IEEE Trans. Ind. Electron.*, vol. 64, no. 9, pp. 6828–6840, Sep. 2017.



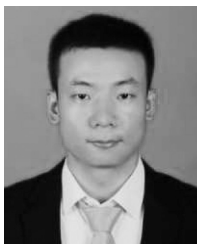
**Fangxing Li** (Fellow, IEEE) is also known as Fran Li. He received the B.S.E.E. and M.S.E.E. degrees from Southeast University, Nanjing, China, in 1994 and 1997, respectively, and the Ph.D. degree from Virginia Tech, Blacksburg, VA, USA, in 2001. He is currently the James W. McConnell Professor of Electrical Engineering and the Campus Director of CURENT with The University of Tennessee, Knoxville, TN, USA. His current research interests include renewable energy integration, demand response, distributed generation and microgrid, energy markets, and power system computing. Since 2020, has been serving as the Editor-in-Chief of IEEE OPEN ACCESS JOURNAL OF POWER AND ENERGY. He was the Past Chair of IEEE PES Power System Operation, Planning and Economics Committee from 2020 to 2021.



**Qiwei Zhang** (Graduate Student Member, IEEE) received the B.S.E.E. degree from North China Electric Power University in 2016, and the M.S.E.E degree from UTK in 2018. He is currently pursuing the Ph.D. degree with the Department of Electrical Engineering and Computer Science, The University of Tennessee, Knoxville, TN, USA. His research interests include cyber security in power systems, power system optimization, and market operation.



**Qingxin Shi** (Member, IEEE) received the B.S. degree from Zhejiang University, China, the M.Sc. degree from the University of Alberta, Canada, in 2011 and 2014, respectively, and the Ph.D. degree from The University of Tennessee, Knoxville, USA, in 2019, where he worked as a Research Assistant Professor from 2019 to 2020. He is currently an Assistant Professor with North China Electric Power University, Beijing, China. His research interests include distribution system resilience and demand response.



**Xiaofei Wang** (Graduate Student Member, IEEE) received the B.S.E.E. degree from North China Electric Power University in 2014, and the M.S.E.E. degree from Wuhan University, China, in 2017. He is pursuing the Ph.D. degree in electrical engineering with The University of Tennessee, Knoxville, TN, USA. His research interests include power system optimization, demand response, and distribution-level market.



**Jinning Wang** (Graduate Student Member, IEEE) received the B.S. and M.S. degrees in electrical engineering from the Taiyuan University of Technology, Taiyuan, China, in 2017 and 2020, respectively. He is currently pursuing the Ph.D. degree in electrical engineering with The University of Tennessee, Knoxville, TN, USA. His research interests include demand response for frequency regulation, renewable integration, and power system control.